Low-temperature mobility of holes in Si/SiGe *p*-channel heterostructures

Doan Nhat Quang*
Department of Physics, Graduate School of Science, Osaka University, 1-1 Machikaneyama, Toyonaka, Osaka 560-0043, Japan

Vu Ngoc Tuoc, Tran Doan Huan,[†] and Pham Nam Phong
Institute of Engineering Physics, Hanoi University of Technology, 1 Dai Co Viet Road, Hanoi, Vietnam
(Received 31 December 2003; published 23 November 2004)

We present a theory of the low-temperature mobility of holes in strained SiGe layers of Si/SiGe *p*-channel heterostructures. Our theory must not be based on the unclear concept of interface impurity charges assumed in the previous calculations, but takes adequate account of the random deformation potential and random piezoelectric field. These appear as effects arising from both lattice mismatch and interface roughness. It is proved that deformation potential scattering may be predominant over the well-known scattering mechanisms such as background doping, alloy disorder, and surface roughness for a Ge content $x \gtrsim 0.2$, while piezoelectric scattering is comparable thereto for $x \gtrsim 0.4$. Our theory turns out to be successful in providing a good quantitative explanation of recent experimental findings not only about the low value of the hole mobility but also its dependence on carrier density as well as its decrease with Ge content.

DOI: 10.1103/PhysRevB.70.195336 PACS number(s): 73.50.Bk, 73.63.Hs

I. INTRODUCTION

Recently, there has been considerable interest in the incorporation of a strained SiGe layer into *p*-channel metal-oxide-semiconductor structures, to give increases in hole mobility and high-field drift velocity.[1–3] However, low-temperature measurements reveal the following striking phenomena. First, the hole mobilities are significantly less than the electron ones. For the two-dimensional electron gas (2DEG) in a Si *n*-channel, peak low-temperature mobilities were reported to be $\sim 4 \times 10^5$ cm^2/V s,[3] while for the two-dimensional hole gas (2DHG) in a strained SiGe *p*-channel, the best mobilities reported not exceeding $\sim 2 \times 10^4$ cm^2/V s.[4–6] Second, the hole mobility is degraded when increasing the Ge content despite a reduction in effective hole mass.[3,7–9]

It has been shown[9–13] that all so-far known scattering mechanisms such as impurity doping, alloy disorder, and surface roughness are unable to account for the earlier experimental data. Therefore, several authors had to invoke the concept of interface charges as a key scattering source at low temperatures. This enables a somewhat satisfactory description of the 2DHG mobility in different strained Si/SiGe heterostructures with a suitable choice of the interface charge density as a fitting parameter.

Nevertheless, there are several drawbacks in the previous theories. First, it was indicated[3,9,10] that the nature of interface charges has been, to date, quite unclear. It was supposed that they can originate from impurity contamination of epitaxial layers during and after growth. The areal impurity density for such an unintentional doping has to be claimed high,[9–13] up to $\sim 10^{11}$ cm^{-2}. The mechanisms for trapping and charging impurities at the heterointerface Si/SiGe are also not clarified.

Second, the decrease observed[3,8] in the low-temperature 2DHG mobility of strained SiGe layers when increasing the Ge content is also still unclear, since alloy disorder was demonstrated[1,7,9–13] likely not to be a dominant scattering source at a low carrier density, e.g., of $\sim 10^{11}$ cm^{-2}. Plews and co-workers[14] have obtained strong experimental evidence that for Si/SiGe/Si systems screening of any scattering potential, whatever its nature, is important, especially, at low values of temperature, carrier density, and Ge content. As a result, with screening included, one cannot fit the observed data simply on the basis of alloy disorder scattering alone, even by taking an unjustifiably large value of the alloy potential.[1,9,13]

Third, it was proved[15–19] that interface roughness gives rise to random variations in all components of the strain field in actual lattice-mismatched heterostructures. As a result, Feenstra and Lutz[16] found that for an *n*-channel Si/SiGe system these fluctuations cause a random nonuniform shift of the conduction band edge. This implies a random deformation potential acting on electrons as a source of scattering, which yields much better agreement with experimental data about the 2DEG mobility[20] than surface roughness scattering does. The existing calculations[9,11,12] of the 2DHG mobility in a *p*-channel Si/SiGe system have been carried out with an extension of the idea of Feenstra and Lutz to the valence band edge, based on the assumption that the deformation potential for holes is almost identical to that for electrons. As seen later, this is in fact invalid.

Finally, in the last years some experimental evidences for piezoelectricity of strained SiGe layers in Si/SiGe systems have been found.[21–24] Further, interface roughness was shown[17–19] to induce a fluctuating density of piezoelectric charges. Scattering by them is to be included in a full treatment of the hole mobility.

Thus, the goal of this paper is to present a theory of the low-temperature 2DHG mobility in strained SiGe layers of Si/SiGe *p*-channel heterostructures. Our theory is to be developed for explaining the experimental data recently reported in Refs. 3, 8, 11, and 12. Moreover, the theory must not be based on the unclear concept of interface impurity charges, but adequately include the possible sources of scattering: alloy disorder, surface roughness, deformation potential, and piezoelectric charges. In particular, the deformation

 ©2004 The American Physical Society

potential for holes must be rigorously derived.

The paper is organized as follows. In Sec. II, we formulate our model and basic equations used to calculate the disorder-limited 2DHG mobility, taking explicitly into account the finiteness of the potential barrier height. In Sec. III, the autocorrelation functions for diverse scattering mechanisms are derived. Section IV is devoted to numerical results and comparison with experiment. Finally, a summary in Sec. V concludes the paper.

II. BASIC FORMULATION

A. Finitely deep triangular quantum well

We are dealing with a 2DHG in a strained SiGe layer as the conduction channel in a Si/SiGe/Si sandwich configuration. This may be the 2DHG located near the upper interface of the strained alloy layer in a gated oxide Si/SiGe heterostructure,[9–11,13] or near its backinterface in a p-channel field-effect structure.[12]

It is well known[25] that scattering by a random field is specified by its autocorrelation function in wave vector space $\langle|U(\mathbf{q})|^2\rangle$. Hereafter, the angular brackets stand for an ensemble average. $U(\mathbf{q})$ is a 2D Fourier transform of the random potential averaged with the envelope wave function of a 2D subband

$$U(\mathbf{q}) = \int_{-\infty}^{+\infty} dz|\zeta(z)|^2 U(\mathbf{q},z). \tag{1}$$

As usual,[9–13] for the holes confined in the SiGe layer, we assume a triangular quantum well (QW) located along the growth direction, e.g., [001] chosen as the z axis, where $z=0$ defines the Si/SiGe interface plane.

The band structure for holes in a strained SiGe layer grown pseudomorphically on a relaxed (001) Si substrate is calculated in Refs. 26–28, including both the strain and quantum confinement effects. It is found[1,26–28] that the top valence band edge is formed by the lowest heavy-hole (HH1) subband, and its energy separation from the first excited subband is large compared to the Fermi level at a rather low hole density. At very low temperatures, the carriers are then assumed to primarily occupy the lowest heavy-hole subband.

It was indicated[29–34] that the potential barrier height in semiconductor heterostructures may play an important role in certain phenomena. For Si/SiGe triangular QWs which we will be dealing with, the barrier height is rather small (a few 0.1 eV). Further, Poisson-Schrödinger simulations showed[11] that the envelope wave function has significant amplitude in the Si barrier layer. Therefore, we must, in general, adopt the realistic model of finitely deep wells.

It has been pointed out[29–31] that for a finitely deep triangular QW, the lowest subband may be very well described by a modified Fang-Howard wave function, proposed by Ando[29]

$$\zeta(z) = \begin{cases} A\kappa^{1/2}\exp(\kappa z/2) & \text{for } z<0, \\ Bk^{1/2}(kz+c)\exp(-kz/2) & \text{for } z>0, \end{cases} \tag{2}$$

in which A, B, c, k, and κ are variational parameters to be determined. Here k and κ are half the wave numbers in the well and the barrier, respectively. A, B, and c are dimensionless parameters given in terms of k and κ through boundary conditions at the interface plane $z=0$ and the normalization. These read as[30,31]

$$A\kappa^{1/2} = Bk^{1/2}c,$$

$$A\kappa^{3/2}/2 = Bk^{3/2}(1-c/2),$$

$$A^2 + B^2(c^2+2c+2) = 1. \tag{3}$$

The energy of the ground-state subband is calculated as a function of the wave numbers k and κ. This involves as parameters the potential barrier height V_0, depletion charge density N_d, and sheet hole density p_s such that[30,31]

$$\begin{aligned} E_0(k,\kappa) = &-\frac{\hbar^2}{8m_z}[B^2k^2(c^2-2c-2)+A^2\kappa^2] + V_0A^2 \\ &+ \frac{4\pi e^2 N_d}{\varepsilon_L}\left[\frac{B^2}{k}(c^2+4c+6) - \frac{A^2}{\kappa}\right] \\ &+ \frac{4\pi e^2 p_s}{\varepsilon_L}\left[\frac{B^4}{4k}(2c^4+12c^3+34c^2+50c+33)\right. \\ &\left.+ \frac{A^4}{2\kappa} - \frac{A^2}{\kappa}\right], \end{aligned} \tag{4}$$

where $m_z=0.28m_e$ means the effective heavy-hole mass in the growth direction, and ε_L is the dielectric constant of the SiGe layer. The effects of image charges are neglected since they are small for carriers in the SiGe channel.[9,13] The wave numbers k and κ in turn are fixed so as to minimize the total energy per electron $E(k,\kappa)$ numerically.[29–31]

In the limiting case of $V_0 \to \infty$, we have $A=0$, $B=1/\sqrt{2}$, $c=0$, and $\kappa \to \infty$, so that Eq. (4) reproduces the lowest-subband energy for an infinitely deep well described by the standard Fang-Howard wave function.[25]

B. Low-temperature hole mobility in a single-subband model

As mentioned earlier, in this paper we are to focus our attention on the explanation of the experimental data compiled in Refs. 3, 8, 11, and 12, where the transport was measured for 2DHGs at very low temperature and rather low carrier density. For the purposes of examining the contributions from various scattering mechanisms and find which are dominant, we will adopt a somewhat simplified model, but one that is accurate enough to capture the features of interest. It has been shown[1,9–13,28,35] that for the case in question it is a good approximation to take into consideration merely intrasubband scattering within the lowest heavy-hole subband HH1, ignoring intersubband scattering. Further, it is found[28] that this subband is isotropic and parabolic over a relatively large range of the 2D wave vector.

As a result, the zero-temperature mobility is determined via the momentum relaxation time

$$\mu = e\tau/m^*, \tag{5}$$

with m^* as an effective in-plane mass.

In what follows, we will, for simplicity, ignore the multiple scattering effects.[35,36] Within the linear transport theory,

the inverse relaxation time for zero temperature is expressed in terms of the autocorrelation function for disorder[28,37,38]

$$\frac{1}{\tau} = \frac{1}{(2\pi)^2 \hbar E_F} \int_0^{2k_F} dq \int_0^{2\pi} d\theta \frac{q^2}{(4k_F^2 - q^2)^{1/2}} \frac{\langle |U(\mathbf{q})|^2 \rangle}{\varepsilon^2(q)}, \tag{6}$$

where $\mathbf{q}=(q,\theta)$ denotes a 2D wave vector in the x-y plane given in polar coordinates, $E_F=\hbar^2 k_F^2/2m^*$ is the Fermi energy, and k_F the Fermi wave number fixed by the hole density: $k_F=\sqrt{2\pi p_s}$. The angle integral appears in Eq. (6) since the autocorrelation function of a random field may have a directional dependence as seen in Eqs. (27) and (30) later.

The dielectric function $\varepsilon(q)$ in Eq. (6) allows for the screening of a scattering potential by the 2DHG, which is, as quoted before, an important effect in the system under consideration. Within the random phase approximation, this is given at zero temperature by[25]

$$\varepsilon(q) = 1 + \frac{q_{\mathrm{TF}}}{q} F_S(q/k)[1 - G(q)] \quad \text{for } q \leqslant 2k_F, \tag{7}$$

with $q_{\mathrm{TF}}=2m^* e^2/\varepsilon_L \hbar^2$ the inverse 2D Thomas-Fermi screening length.

The screening form factor $F_S(q/k)$ in Eq. (7) accounts for the extension of hole states along the growth direction, defined by

$$F_S(q/k) = \int_{-\infty}^{+\infty} dz \int_{-\infty}^{+\infty} dz' |\zeta(z)|^2 |\zeta(z')|^2 e^{-q|z-z'|}. \tag{8}$$

By means of Eq. (2) for the lowest-subband wave function, this is expressed as a function of the dimensionless wave numbers in the 2DHG plane $t=q/k$ and the barrier layer $a=\kappa/k$ by[31]

$$\begin{aligned} F_S(t) = {} & \frac{A^4 a}{t+a} + 2A^2 B^2 a \frac{2 + 2c(t+1) + c^2(t+1)^2}{(t+a)(t+1)^3} \\ & + \frac{B^4}{2(t+1)^3}[2(c^4 + 4c^3 + 8c^2 + 8c + 4) + t(4c^4 + 12c^3 \\ & + 18c^2 + 18c + 9) + t^2(2c^4 + 4c^3 + 6c^2 + 6c + 3)]. \end{aligned} \tag{9}$$

For $V_0 \to \infty$, Eq. (9) reproduces the well-known formula for the screening form factor.[25]

Finally, the function $G(q)$ appears in Eq. (7) to allows for the local field corrections associated with the many-body interaction in the 2DHG. Within Hubbard's approximation, in which merely the exchange effect is included, it holds[39]

$$G(q) = \frac{q}{2(q^2 + k_F^2)^{1/2}}. \tag{10}$$

At very low (zero) temperatures the holes in a strained SiGe layer are expected to experience the following possible scattering mechanisms: (i) alloy disorder due to random fluctuations in the constituent, (ii) surface roughness due to random fluctuations in the position of the potential barrier, (iii) deformation potential, and (iv) piezoelectric charges. The latter two are random effects arising from combination of lattice mismatch and interface roughness (not confused with relevant scatterings due to acoustic waves).[17–19] The total relaxation time is then determined by

$$\frac{1}{\tau_{\mathrm{tot}}} = \frac{1}{\tau_{\mathrm{AD}}} + \frac{1}{\tau_{\mathrm{SR}}} + \frac{1}{\tau_{\mathrm{DP}}} + \frac{1}{\tau_{\mathrm{PE}}}. \tag{11}$$

III. AUTOCORRELATION FUNCTIONS FOR SCATTERING MECHANISMS

A. Alloy disorder

As evidently seen from Eq. (6), in our calculation of the disorder-limited mobility the autocorrelation function in wave vector space $\langle |U(\mathbf{q})|^2 \rangle$ takes a key role. Thus, we ought to specify it for the earlier-mentioned sources of scattering.

For the 2DHG located on the side of a SiGe layer, the autocorrelation function for alloy disorder scattering is supplied in the form[29,30]

$$\langle |U_{\mathrm{AD}}(\mathbf{q})|^2 \rangle = x(1-x) u_{\mathrm{al}}^2 \Omega_0 \int_0^L dz \zeta^4(z), \tag{12}$$

where x denotes the Ge content, u_{al} is the alloy potential, L the SiGe layer thickness. The volume occupied by one alloy atom is given by $\Omega_0=a_{\mathrm{al}}^3(x)/8$, with $a_{\mathrm{al}}(x)$ the lattice constant of the alloy.

By means of Eq. (2) for the lowest-subband wave function, this is rewritten in terms of the dimensionless wave number in the well $b=kL$ as follows:

$$\begin{aligned} \langle |U_{\mathrm{AD}}(\mathbf{q})|^2 \rangle = {} & x(1-x) u_{\mathrm{al}}^2 \Omega_0 \frac{B^4 b^2}{L}[c^4 p_0(2b) + 4c^3 p_1(2b) \\ & + 6c^2 p_2(2b) + 4c p_3(2b) + p_4(2b)]. \end{aligned} \tag{13}$$

Hereafter, we have introduced auxiliary functions $p_l(v)$ ($l=0-4$) of the variables v and b, defined by

$$p_l(v) = \frac{b^l}{v^{l+1}} \left(1 - e^{-v} \sum_{j=0}^{l} \frac{v^j}{j!} \right), \tag{14}$$

with l an integer.

In the limiting case of infinitely deep QWs ($B=1/\sqrt{2}$, $c=0$) in which the SiGe thickness is so large that the hole state is localized essentially within the SiGe layer ($b>1$), Eq. (13) reproduces the autocorrelation function for alloy disorder employed previously.[9,12] In the opposite case of a thin SiGe layer ($b<1$), the hole state overlaps merely in part with the alloy, so that the probability of alloy disorder scattering becomes smaller.

B. Surface roughness

We are now treating scattering of confined charge carriers from a rough potential barrier of a finite height V_0. The scattering potential is due to fluctuations in the position of the barrier. The average scattering potential in wave vector space is fixed by the value of the envelope wave function at the barrier plane ($z=0$) according to[25]

$$U_{\mathrm{SR}}(\mathbf{q}) = V_0 |\zeta(0)|^2 \Delta_{\mathbf{q}}, \tag{15}$$

where $\Delta_{\mathbf{q}}$ is a Fourier transform of the interface profile.

To estimate the average potential for surface scattering specified by Eq. (15) with the use of a variational wave function, we are to adopt the following relation:

$$V_0|\zeta(0)|^2 = \int_0^\infty dz|\zeta(z)|^2 \frac{\partial V}{\partial z}. \quad (16)$$

Here, $V(z)$ means the Hartree potential induced by the depletion charge density and the hole density distribution, given by (Ref. 29):

$$V(z) = \frac{4\pi e^2}{\varepsilon_L} N_d z + \frac{4\pi e^2}{\varepsilon_L} p_s \int_0^z dz' \int_{z'}^\infty dz'' |\zeta(z'')|^2. \quad (17)$$

It should be remarked that Eq. (16) is similar to the relation due to Matsumoto and Uemura.[25] However, the former involves, on the left-hand side, the wave function at the barrier plane $\zeta(0)$, whereas the latter its derivative $d\zeta(0)/dz$. Accordingly, the former is exact and applicable for any value of V_0, whereas the latter is approximate and applicable merely for large enough V_0.

Upon inserting the lowest-subband wave function from Eq. (2) into Eqs. (16) and (17), we have

$$V_0|\zeta(0)|^2 = \frac{4\pi e^2}{\varepsilon_L} B^2 \left[N_d(c^2 + 2c + 2) + \frac{p_s}{2} B^2 (c^4 + 4c^3 + 8c^2 + 8c + 4) \right]. \quad (18)$$

With the help of Eqs. (15) and (18), we are able to obtain the autocorrelation function for surface roughness scattering in finitely deep triangular QWs in the form

$$\langle |U_{\rm SR}(\mathbf{q})|^2 \rangle = \left(\frac{4\pi e^2}{\varepsilon_L} \right)^2 B^4 \left[N_d(c^2 + 2c + 2) + \frac{p_s}{2} B^2 (c^4 + 4c^3 + 8c^2 + 8c + 4) \right]^2 \langle |\Delta_{\mathbf{q}}|^2 \rangle. \quad (19)$$

For $V_0 \to \infty$, this reproduces the probability for surface roughness scattering in an infinitely deep well.[12,13,25]

Thus, the obtained autocorrelation function depends on the spectral distribution of the interface profile. For simplicity, this has usually been chosen in a Gaussian form.[25] However, no real justification has been provided for this assumption. For the case of Si/SiGe heterostructures, Feenstra and co-workers[20] measured the surface morphology by means of atomic force microscopy and indicated that the Fourier spectrum for the surface roughness contains three distinct components, each described better by a power-law distribution

$$\langle |\Delta_{\mathbf{q}}|^2 \rangle = \frac{\pi \Delta^2 \Lambda^2}{(1 + q^2 \Lambda^2 / 4n)^{n+1}}. \quad (20)$$

Here Δ is the roughness amplitude, Λ is a correlation length, and n is an exponent specifying the falloff of the distribution at large wave numbers.

C. Deformation potential

Next, we turn to the study of scattering mechanisms which appear as a result of combination of the lattice mismatch and surface roughness effects. In what follows, we are concerned with a SiGe layer grown pseudomorphically on a (001) Si substrate.

It is well known[40,41] that if the Si/SiGe interface is ideal, i.e., absolutely flat, the strain field in the SiGe layer is uniform and has vanishing off-diagonal components. Its in-plane component is defined in terms of the lattice constants of the Si and alloy layers by

$$\epsilon_{\parallel}(x) = \frac{a_{\rm Si} - a_{\rm al}(x)}{a_{\rm al}(x)}, \quad (21)$$

where the Ge content x dependence is explicitly indicated. The strain in the alloy is demonstrated to bring about a shift of the band edges of its conduction and valence bands.[42–46]

As mentioned before, because of interface roughness the strain field in the SiGe layer is subjected to random variations and its off-diagonal components become nonzero.[15–19] These fluctuations in turn give rise to a random nonuniform shift of the band edges. This means that the electrons in the conduction band and the holes in the valence one must experience a random deformation potential. In the existing calculations of the 2DHG mobility it has been assumed[9,11,12] that the perturbating potential for holes in the SiGe layer is almost identical to that for electrons, having one and the same shape described by Eq. (22) later, only with a different value of the coupling constant Ξ_u.

Nevertheless, this assumption is invalid. Indeed, with the use of the strain Hamiltonian for a semiconductor crystal of cubic symmetry, it has been proved (see, e.g., Refs. 42–46) that the impacts of the strain field on electrons and on holes are quite different. This field is calculated within a simple approach to cubic symmetry,[18] in which the deviation from isotropy is taken into account in terms of an anisotropy ratio.[47] The volume dilation is then found unaffected by strain fluctuations, being uniform in space. As a result, the deformation potential for electrons in the conduction band is fixed by a single diagonal component of the strain field[16,42–44]

$$U_{\rm DP}^{(c)} = \Xi_u \epsilon_{zz}, \quad (22)$$

while that for holes in the valence band is fixed by all its components[43–46]

$$[U_{\rm DP}^{(v)}]^2 = \frac{b_s^2}{2}[(\epsilon_{xx} - \epsilon_{yy})^2 + (\epsilon_{yy} - \epsilon_{zz})^2 + (\epsilon_{zz} - \epsilon_{xx})^2] + d_s^2[\epsilon_{xy}^2 + \epsilon_{yz}^2 + \epsilon_{zx}^2], \quad (23)$$

with b_s and d_s as shear deformation potential constants. Here ϵ_{ij} denote the roughness-induced variations in the strain field components. Therefore, in our calculation of the 2DHG mobility limited by deformation potential scattering, we will adopt Eq. (23) rather than Eq. (22) assumed previously.[9,11,12]

Upon putting the strain fluctuations ϵ_{ij} derived in Refs. 17 and 18 into Eq. (23), we readily get a 2D Fourier transform for the perturbating potential for holes in the SiGe layer as follows:

$$U_{\rm DP}^{(v)}(\mathbf{q},z)=\frac{\alpha\epsilon_{\|}}{2}q\Delta_{\mathbf{q}}e^{-qz}\left[\frac{3}{2}[b_s(K+1)]^2(1+\sin^4\theta+\cos^4\theta)+\left(\frac{d_sG}{4c_{44}}\right)^2(1+\sin^2\theta\cos^2\theta)\right]^{1/2}, \tag{24}$$

for $0\leqslant z\leqslant L$ and is zero elsewhere, with L the SiGe layer thickness, and $\mathbf{q}=(q,\theta)$ a 2D wave vector in polar coordinates. Here α is the anisotropy ratio of the alloy

$$\alpha=2\frac{c_{44}}{c_{11}-c_{12}}; \tag{25}$$

K and G are its elastic constants

$$K=2\frac{c_{12}}{c_{11}},\quad G=2(K+1)(c_{11}-c_{12}), \tag{26}$$

with c_{11}, c_{12}, and c_{44} as its elastic stiffness constants.

Upon averaging Eq. (24) by means of the lowest-subband wave function from Eq. (2), we may represent the autocorrelation function for deformation potential scattering of holes in terms of the dimensionless variables $t=q/k$ and $b=kL$ by

$$\langle|U_{\rm DP}^{(v)}(\mathbf{q})|^2\rangle=\left(\frac{B^2b^2\alpha\epsilon_{\|}}{2L}\right)^2t^2[c^2p_0(b+bt)+2cp_1(b+bt)+p_2(b+bt)]^2\left[\frac{3}{2}[b_s(K+1)]^2(1+\sin^4\theta+\cos^4\theta)+\left(\frac{d_sG}{4c_{44}}\right)^2(1+\sin^2\theta\cos^2\theta)\right]\langle|\Delta_{\mathbf{q}}|^2\rangle, \tag{27}$$

in which $p_l(v)$ $(l=0-2)$ are functions given by Eq. (14) with the variable $v=b+bt$.

D. Piezoelectric charges

As already mentioned in Sec. I, some experimental evidences for piezoelectricity of the strained SiGe layer in a Si/SiGe heterostructure have been found.[21–24] However, if the Si/SiGe interface is ideal, the strain field in the alloy has vanishing off-diagonal components, so that the SiGe layer exhibits neither a piezoelectric polarization nor any piezoelectric field.

In fact, because of surface roughness the off-diagonal components of the strain field in the SiGe layer of an actual Si/SiGe system become nonzero and randomly fluctuating.[15–19] Therefore, they induce a piezoelectric polarization and a corresponding fluctuating density of piezoelectric charges, which are bulklike distributed in a rather narrow region inside of the alloy and near the Si/SiGe interface.[17–19]

These charges in turn create a random piezoelectric field. The potential energy for a hole of charge e in this field is described by a 2D Fourier transform as follows:[17,18]

$$U_{\rm PE}(\mathbf{q},z)=\frac{3\pi ee_{14}G\alpha\epsilon_{\|}}{4\varepsilon_Lc_{44}}q\Delta_{\mathbf{q}}F_{\rm PE}(q,z;L)\sin 2\theta, \tag{28}$$

where e_{14} is the piezoelectric constant of the strained SiGe layer. The form factor for the piezoelectric potential in Eq. (28) is supplied by[18]

$$F_{\rm PE}(q,z;L)=\frac{1}{2q}\begin{cases}e^{qz}(1-e^{-2qL}) & \text{for } z<0,\\ e^{-qz}(1+2qz)-e^{-q(2L-z)}, & \text{for } 0\leqslant z\leqslant L,\\ 2qLe^{-qz} & \text{for } z>L.\end{cases} \tag{29}$$

Upon averaging Eqs. (28) and (29) by means of the lowest-subband wave function from Eq. (2), we arrive at the autocorrelation function for piezoelectric scattering in the form

$$\langle|U_{\rm PE}(\mathbf{q})|^2\rangle=\left(\frac{3\pi ee_{14}G\alpha\epsilon_{\|}}{8\varepsilon_Lc_{44}}\right)^2F_{\rm PE}^2(q/k)\sin^2 2\theta\langle|\Delta_{\mathbf{q}}|^2\rangle. \tag{30}$$

Here the weighted piezoelectric form factor is defined as a function of $t=q/k$ by

$$F_{\rm PE}(t)=\frac{A^2a}{t+a}(1-e^{-2bt})+B^2b\left\{\frac{2c^2t}{t+1}+\frac{4ct}{(t+1)^2}+\frac{4t}{(t+1)^3}+c^2(1-2bt)p_0(b+bt)+2c(1+ct-2bt)p_1(b+bt)+(1+4ct-2bt)p_2(b+bt)+2tp_3(b+bt)-e^{-2bt}[c^2p_0(b-bt)+2cp_1(b-bt)+p_2(b-bt)]\right\}, \tag{31}$$

where as before $a=\kappa/k$, and $p_l(v)$ $(l=0-3)$ are given by Eq. (14) with the variables $v=b\pm bt$.

Thus, within the realistic model of finitely deep triangular QWs described by the modified Fang-Howard wave function (2), we may rigorously derive the autocorrelation functions in an analytic form for the scattering mechanisms of interest. These are supplied by Eqs. (13), (19), (27), and (30) for alloy disorder, surface roughness, deformation potential, and piezoelectric charges, respectively. It is to be noted that the latter two show up in a dependence not only on the magnitude of the wave vector but its polar angle as well.

IV. RESULTS AND DISCUSSIONS

A. Choice of input parameters

In this section, we are trying to apply the foregoing theory to explain the experimental data[3,8,11,12] about the low-temperature transport of holes located near an interface of the strained SiGe layer as the conduction channel in a Si/SiGe/Si sandwich configuration.

For numerical results, we have to specify parameters appearing in the theory as input. As always with mobility calculations, one has many adjustable fitting parameters. In order that the justification of our theory is so independent as possible of the choice of fitting parameters, these are to be deduced from measurements of other physical properties than the hole mobility.

The lattice constants, elastic stiffness constants, dielectric constants, and shear deformation potentials for Si and Ge are

TABLE I. Material parameters used: a as the lattice constant (Å), c_{ij} as the elastic stiffness constants (10^{10} Pa), ε_L as the dielectric constant, and b_s and d_s as the shear deformation potential constants (eV).

Material	a	c_{11}	c_{12}	c_{44}	ε_L	b_s	d_s
Si	5.430	16.6	6.39	7.96	11.7	–2.35	–5.32
Ge	5.658	12.85	4.83	6.80	15.8	–2.55	–5.50

taken from Refs. 44 and 48 and listed in Table I. The corresponding constants for the alloy are estimated according to the virtual crystal approximation[49] except the lattice constant given by an empirical rule, Eq. (32) later. The potential barrier height of triangular QWs for holes is the valence band offset between the Si and SiGe layers, which increases nearly linearly with the Ge content x as $V_0=0.74x$ eV.[1]

For the x dependence of the lattice constant of a SiGe alloy, we use the experimental data, approximated analytically by[50,51]

$$a_{\rm al}(x) = a_{\rm Si}(1-x) + a_{\rm Ge}x - \gamma x(1-x), \tag{32}$$

with a parameter $\gamma=1.88\times10^{-2}$ Å.

It is to be noted[1] that the built-in biaxial compressive strain in a SiGe layer produces a reduction in its in-plane heavy-hole mass, thus leading to an increase of the 2DHG mobilities. The x dependence of the mass is given by a linear interpolation to fit to the experimental data[52–54]

$$m^*(x)/m_{\rm e} = 0.44 - 0.42x. \tag{33}$$

We are now concerned with choosing the coupling constants of interest. The alloy potential was taken as equal to $u_{\rm al}=0.6$ eV.[12,13,52] The value of the piezoelectric constant $e_{14}=1.6\times10^{-2}$ C/m^2 was extracted from power loss measurement[21] for a SiGe alloy with a Ge content $x=0.2$. Furthermore, in view of the fact that piezoelectricity of the SiGe alloy in a lattice-mismatched structure is induced by strain, for a crude estimate we scale the relevant coupling constant by the strain ratio. Then, for the x dependence of the piezoelectric constant it holds

$$e_{14}(x) = 1.6\times10^{-2}\frac{\epsilon_{\parallel}(x)}{\epsilon_{\parallel}(0.2)}({\rm C/m^2}). \tag{34}$$

It should be kept in mind that all scattering mechanisms under consideration depend, in general, strongly on the Ge content because not only the effective mass but, as seen earlier, the lattice mismatch and the piezoelectric constant depend on it.

Next, we turn to the characteristics of the interface profile. It has recently been shown[16,20] that for a Si/SiGe heterostructure, the most important component of the surface roughness is connected with elastic strain relaxation in the channel layer. Moreover, the experimental data about the electron mobility in Si/SiGe n-channel heterostructures suggested[16,20] that the correlation length of this component is $\Lambda\lesssim300$ Å, its roughness amplitude $\Delta=5-15$ Å, and its exponent of the power-law distribution $n\lesssim4$, varying remarkably from device to device. For our numerical calculations, we take $\Lambda=290$ Å, $\Delta=15.5$ Å, and $n=4$. The somewhat large value of the roughness amplitude may be explained in terms of the segregation and clustering effects, which are indicated[55,56] to be the main reasons for roughening of the interfaces in a strained layer.

It should be noted that our choice of the interface profile characteristics satisfies the condition

$$\Delta/\Lambda \ll 1. \tag{35}$$

This is claimed[16] in order that the theory of roughness-induced fluctuations in strain[15–19] and, hence, that of deformation potential and piezoelectric scatterings presented in Sec. III, are justified.

B. Numerical results and comparison with experiment

By means of Eqs. (5) and (6), we have calculated the low-temperature 2DHG mobilities limited by different scattering mechanisms: alloy disorder $\mu_{\rm AD}$, surface roughness $\mu_{\rm SR}$, deformation potential $\mu_{\rm DP}$, piezoelectric charges $\mu_{\rm PE}$, and overall mobility $\mu_{\rm tot}$; employing Eqs. (13), (19), (27), (30), and (11), respectively. For device applications, one is interested in their variation with hole density p_s and Ge content x. The theoretical results are to be compared with recent experimental data.[3,8,11,12]

As a first illustration, we are dealing with the Si/SiGe sample studied in Ref. 12 This is specified by a fixed Ge content $x=0.2$ and a depletion charge[10] $N_d\sim5\times10^{11}$ cm^{-2}, while the hole density p_s is varying.

We need to estimate the effect due to the finiteness of the potential barrier height on the hole mobilities. This is to be measured by the ratio between the values of a partial mobility calculated with a finite and an infinite barrier

$$Q = \mu^{\rm fin}/\mu^{\rm infin}. \tag{36}$$

The mobility ratios for the various scattering sources are depicted in Fig. 1 versus sheet hole density ranging from $p_s=1\times10^{11}-5.5\times10^{11}$ cm^{-2} for a SiGe layer thickness $L=200$ Å.

The partial 2DHG mobilities of the sample under study are plotted versus hole density from $p_s=1.5\times10^{11}-5.5\times10^{11}$ cm^{-2} in Fig. 2, where the 4 K experimental data reported in Ref. 12 is reproduced for a comparison. In addition, these are plotted in Fig. 3 versus alloy layer thickness from $L=20-90$ Å for a hole density $p_s=2\times10^{11}$ cm^{-2}.

From the lines thus obtained we may draw the following conclusions.

(i) Figure 1 reveals that the model of infinitely deep triangular QWs overestimates surface roughness and piezoelectric scatterings: $Q_{\rm SR}, Q_{\rm PE}>1$, while this underestimates alloy disorder and deformation potential scatterings: $Q_{\rm AD}, Q_{\rm DP}<1$. The finite-barrier effect is found to be small compared with

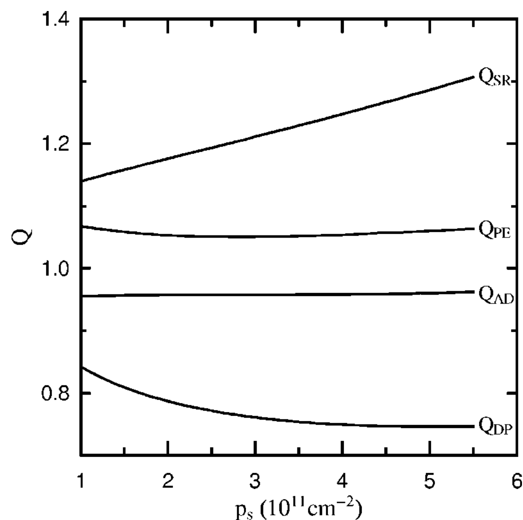

FIG. 1. Ratio $Q=\mu^{fin}/\mu^{infin}$ between the 2DHG mobilities, calculated with a finite and an infinite potential barrier, vs sheet hole density p_s for various scattering mechanisms: alloy disorder Q_{AD}, surface roughness Q_{SR}, deformation potential Q_{DP}, and piezoelectric charges Q_{PE}. The triangular QW is made from $Si/Si_{0.8}Ge_{0.2}$ with a barrier height $V_0=0.148$ eV and a SiGe layer thickness $L=200$ Å.

the one in the case of square QWs,[18] where the mobility ratios may become very large, e.g., $Q_{SR}\gtrsim 10$ for a narrow square well of a thickness $\lesssim 100$ Å. The overestimation of surface scattering is distinct from the earlier statement[29] concerning GaAs/AlGaAs triangular QWs that surface scattering is independent of their barrier height because the overlapping of the envelope wave function with the barrier was neglected.

(ii) It is clearly seen from Fig. 2 that the calculated overall mobility $\mu_{tot}(p_s)$ almost coincides with the 2DHG mobility obtained experimentally[12] in the region of carrier densities

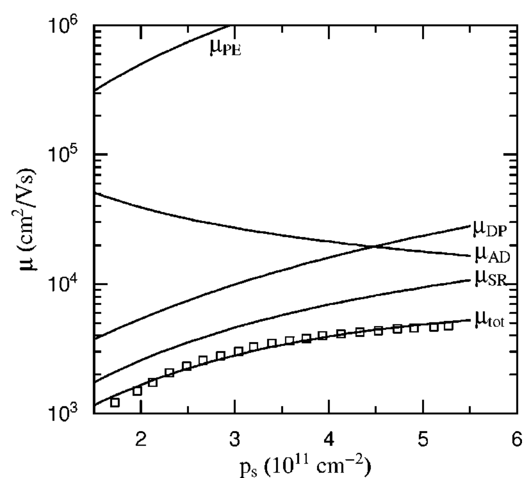

FIG. 2. Different 2DHG mobilities of the $Si/Si_{0.8}Ge_{0.2}$ QW in Fig. 1 vs hole density p_s. The solid lines show the calculated mobilities limited by: alloy disorder μ_{AD}, surface roughness μ_{SR}, deformation potential μ_{DP}, piezoelectric charges μ_{PE}, and overall μ_{tot}. The 4 K experimental data reported in Ref. 12 are marked by squares.

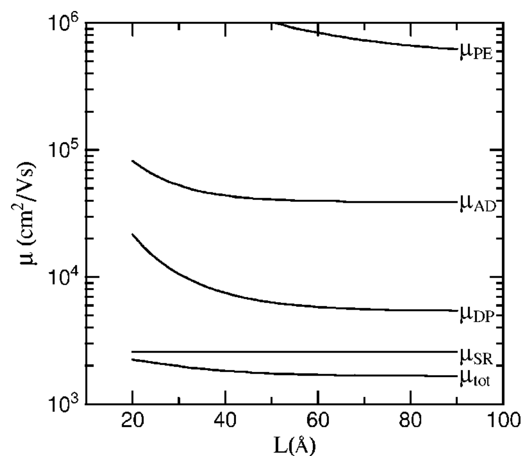

FIG. 3. Different 2DHG mobilities of the $Si/Si_{0.8}Ge_{0.2}$ QW in Fig. 1 vs SiGe thickness L. The interpretation is the same as in Fig. 2.

used. This exhibits a significant increase when raising the hole density from $p_s=1.5\times10^{11}-5.5\times10^{11}$ cm^{-2}. The functions $\mu_{SR}(p_s)$, $\mu_{DP}(p_s)$, and $\mu_{PE}(p_s)$ are found to increase with a rise of p_s, whereas $\mu_{AD}(p_s)$ to decrease. The sharp contrast between the variation tendencies with p_s of the experimental data $\mu_{expt}(p_s)$ and $\mu_{AD}(p_s)$ implies that in terms of alloy disorder alone one cannot explain the hole density dependence of the measured mobility. Moreover, it has been pointed out that in terms of alloy disorder one cannot understand even qualitatively its dependence on growth temperature[1,2,7] and Si cap thickness.[2]

It is worthy to recall[9–13] that with screening included all the so far-known scattering mechanisms (impurity doping, alloy disorder, and surface roughness) are unable to explain the observed data about the 2DHG mobility in strained SiGe alloys. Therefore, the existing theories had to invoke the unclear concept of interface charged impurities with a high fitting density, up to $\sim10^{11}$ cm^{-2}, which is equivalent to an intentional doping at an intermediate level.

Moreover, in several cases the interface had to be assumed to be quite rough with a small exponent of the power-law distribution, a large ratio between the roughness amplitude and correlation length and a small value of the latter, e.g., $n\sim2$, $\Delta/\Lambda\sim1$, $\Lambda\sim7$ Å (Ref. 11), and $n\sim1$, $\Delta/\Lambda\sim0.5$, $\Lambda\sim19$ Å (Ref. 12). With these large values of Δ/Λ the theory of deformation potential scattering adopted in the earlier calculations[9,11,12] may fail to be valid. In addition, in the case of short correlation lengths, the functions $\mu_{SR}(p_s)$ and $\mu_{DP}(p_s)$ were found to decrease with a rise of p_s,[1,9] which is in opposite to our result. However, such surface morphologies seem to be suspect.[3]

(iii) An examination of the different lines in Fig. 2 indicates that for low carrier densities $p_s<4\times10^{11}$ cm^{-2}, surface roughness and deformation potential scatterings are dominant mechanisms, whereas alloy disorder one is less relevant, which is in accordance with the previous theories.[1,7,9,10,13] For higher densities $p_s\gtrsim4\times10^{11}$ cm^{-2} the latter is comparable with the former two. Furthermore, piezoelectric scattering is found to be negligibly weak at a rather low Ge content $(x=0.2)$.

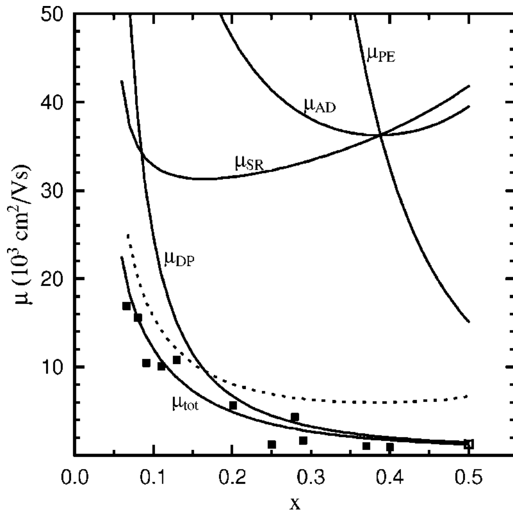

FIG. 4. Different 2DHG mobilities of the $Si/Si_{1-x}Ge_x$ triangular QW vs Ge content x under a SiGe layer thickness $L=200$ Å and a hole density $p_s=2\times10^{11}$ cm^{-2}. The interpretation is the same as in Fig. 2. The dashed line refers to the calculation based on alloy disorder alone without screening and with an alloy potential $u_{al}=0.74$ eV. The 4 K experimental data reported in Refs. 3 and 8 are marked by filled squares, and in Ref. 11 by open one. [Note the ordinate axis scale is distinct from that in Figs. 2 and 3.]

(iv) It follows from Fig. 3 that the hole mobilities depend weakly on the SiGe layer thickness. For $L\gtrsim60$ Å, they are almost independent thereof.

Next, we turn to treating the Ge content dependence of the partial 2DHG mobilities in a $Si/Si_{1-x}Ge_x$ triangular QW. These are plotted versus Ge content varying from $x=0.05$ to 0.5 for a fixed carrier density $p_s=2\times10^{11}$ cm^{-2} and a depletion charge[10] $N_d\sim5\times10^{10}$ cm^{-2} in Fig. 4, where the 4 K experimental data[3,8,11] are reproduced for a comparison. There is also presented the hole mobility reported in Ref. 3, which was calculated simply on the basis of alloy disorder scattering alone by neglecting screening and taking a larger value of the alloy potential: $u_{al}=0.74$ eV. As quoted earlier, the SiGe layer thickness is of minor importance, so we may chose some value, say $L=200$ Å.

From the solid lines obtained in Fig. 4 we may draw the following conclusions.

(i) The calculated overall mobility $\mu_{tot}(x)$ offers a good quantitative description of the pronounced monotonic decrease of the experimentally observed 2DHG mobility when raising Ge content.[3,7,9] It is to be noted that most earlier theoretical studies[27,57] predicted, in contrast, an increase of the hole mobility with higher x, based on the strain-induced reduction in the effective hole mass.

(ii) The functions $\mu_{DP}(x)$ and $\mu_{PE}(x)$ show up in a fast monotonic decrease, whereas $\mu_{AD}(x)$ and $\mu_{SR}(x)$ in a minimum. It is seen from Eqs. (27), (30), and (34) that the probabilities for deformation potential and piezoelectric scatterings depend quadratically on the lattice mismatch $\epsilon_{\parallel}(x)$, and the latter also depends quadratically on the piezoelectric constant $e_{14}(x)$. Since $\epsilon_{\parallel}(x)$ and $e_{14}(x)$ increase when raising x, the fast increase in the scattering probabilities overwhelms the reduction in the effective hole mass with higher x, thus leading to an overall decrease of $\mu_{DP}(x)$ and $\mu_{PE}(x)$. In addition, the distinction between the variation tendencies with x of the experimental data $\mu_{expt}(x)$ and $\mu_{AD}(x)$ implies that in terms of alloy disorder alone one cannot explain the Ge content dependence of the measured mobility.

(iii) Surface roughness scattering is found to be most important at a very low Ge content $x\sim0.05$, while the deformation potential scattering to dominate the overall hole mobility $\mu_{tot}(x)$ for $x>0.1$, leading to its decrease with higher x. As mentioned earlier, the effect due to piezoelectric charges increases very rapidly with a rise of x. So, this is negligibly small for $x\lesssim0.3$, however, this becomes comparable with alloy disorder and surface roughness scatterings for $x\gtrsim0.4$, and with the deformation potential one at a higher $x\sim0.5$.

It is worth mentioning that the roughness amplitude is expected[55] to be increased with strain and, hence, with Ge content x. Therefore, with an increase of x the roughness amplitude-dependent scattering mechanisms such as surface roughness, deformation potential and piezoelectric charges become more important compared to alloy disorder one.

(iv) An inspection of the dashed line in Fig. 4 indicates that the 2DHG mobility calculation in Ref. 3, based on alloy disorder scattering alone, results in a shallow minimum at $x\sim0.4$ and, hence, is unable to supply a satisfactory description of the observed data. In particular, for $x=0.5$ this calculation even without screening and with a large alloy potential ($u_{al}=0.74$ eV) gives: $\mu_{AD}^{unscr}=6.7\times10^3$ cm^2/V s, which is found too large to explain the 4 K experimental data reported in Ref. 11, which our theory may give: $\mu_{tot}\sim\mu_{expt}=1.2\times10^3$ cm^2/V s. The situation becomes much worse when screening included: $\mu_{AD}^{scr}=3.5\times10^4$ cm^2/V s.

C. Validity of the single-subband model

To end this section, we verify the validity of the assumptions made in our hole mobility calculation.

First, it should be emphasized that our theory of hole transport is to be developed for 2DHGs studied experimentally in Refs. 3, 8, 11, and 12; namely at very low temperature ($\lesssim4$ K) and rather low carrier density ($\lesssim5\times10^{11}$ cm^{-2}), which correspond to small values of the energies of interest: $k_BT\lesssim0.3$ meV and $E_F\lesssim4$ meV. At the so low temperatures phonon scattering is obviously negligibly weak.[11,13,28]

As quoted before, it follows from the band structure calculation[1,26–28] for a strained SiGe layer grown on relaxed (001) Si that the ground-state subband is the lowest heavy-hole HH1. In addition, Laikhtman and Kiehl[28] have shown that the heavy-hole–light-hole band splitting HH1–LH1 and the subband splitting HH1–HH2 due to the strain and quantum confinement effects are both larger than 70 meV. These splittings turn out to be at least one order of magnitude greater than the thermal and Fermi energies. Therefore, the assumption of intraband scattering within the lowest heavy-hole subband HH1 is firmly confirmed.[1,9–13,28,35] Further, Leadley and co-workers[11] indicate that the single-subband model is still a reasonable approximation for strained $Si_{0.5}Ge_{0.5}$ at higher temperature (300 K) and higher carrier density (3×10^{12} cm^{-2}).

It should be remarked that the earlier scattering model is to be distinguished from the one employed in the calculation[58–60] of the hole mobility in a strained Si layer at high temperature (~ 300 K) and high carrier density ($\sim 5 \times 10^{12}$ cm^{-2}). In this case, phonon scattering is important. The band structure calculation due to Fischetti and co-workers[60] reveals that the ground-state subband is the lowest heavy-hole HH1 or light-hole LH1 for compressive or tensile stress, respectively. Moreover, the subband splittings are found to be of the order of the thermal and Fermi energies. Therefore, a multisubband model is mandatory.

Further, the existing band structure calculation[28] also shows that for a strained SiGe layer on relaxed (001) Si, the subbands are strongly nonparabolic and anisotropic except for the lowest heavy-hole one. The subband HH1 is isotropic and parabolic over a relatively large range of the 2D wave vector, which corresponds to a large range of the carrier density, up to 10^{13} cm^{-2}.

At last, based on the assumption of intraband scattering within the isotropic parabolic subband HH1, we have been successful in the quantitative explanation of the observed dependences of the hole mobility on Ge content[3,8,11] as well as carrier density.[12] This success provides a real justification for the adopted model.

V. SUMMARY

In this paper we have presented a theory of the low-temperature mobility of holes in strained SiGe layers of Si/SiGe p-channel heterostructures, getting rid of the unclear concept of interface impurity charges. Instead, we took adequate account of the random deformation potential and random piezoelectric field in actual strained SiGe layers.

We have proved that the 2DHG transport in an undoped systems is, in general, governed by the following scattering mechanisms: alloy disorder, surface roughness, deformation potential, and piezoelectric charges. The latter two arise as a combined effect from lattice mismatch and interface roughness.

Scatterings by deformation potential and piezoelectric charges rapidly increase when raising the Ge content x. Thus, the former may become dominant for $x \gtrsim 0.2$, whereas the latter may be one of the principal processes limiting the hole mobility for $x \gtrsim 0.4$.

In the regions of hole density and Ge content in use, surface roughness and deformation potential scatterings are found to be most important. In combination with the other sources of scattering, these enable a good quantitative explanation of the recent experimental findings both about the dependence of the low-temperature 2DHG mobility on hole density and its decrease with Ge content as well.

It is worth mentioning the counteracting strain effects in Si/SiGe p-channel heterostructures. The strain leads to the lifting of the degeneracy of the valence band of SiGe and, hence, to a suppression of intersubband scattering and a reduction of the effective mass, so enhancing the hole mobility. On the other hand, the roughness-induced strain fluctuations give rise to new scattering sources, viz. deformation potential and piezoelectric charges, so reducing the mobility.

ACKNOWLEDGMENTS

The authors would like to thank Professor M. Saitoh, Department of Physics, Osaka University, Japan for valuable discussion and Professor T. E. Whall, Department of Physics, University of Warwick, UK for useful communications. One of the authors (D.N.Q.) acknowledges support from the Japan Society for the Promotion of Science, under which this work was done.

*Present address: Center for Theoretical Physics, Vietnamese Academy of Science and Technology, P.O. Box 429, Boho, Hanoi 10000, Vietnam.

†Present address: Department of Physics, Florida State University, Tallahassee, Florida 32306-4350.

[1] T.E. Whall and E.H.C. Parker, J. Phys. D **31**, 1397 (1998).

[2] T.E. Whall and E.H.C. Parker, Thin Solid Films **368**, 297 (2000).

[3] F. Schäffler, Semicond. Sci. Technol. **12**, 1515 (1997); in *Properties of Silicon, Germanium, and SiGe*, edited by E. Kasper and K. Lyutovich (IEE, London, 2000), Sec. 5.2.

[4] T. Mishima, C.W. Fredriksz, G.F.A. van de Walle, D.J. Gravesteijn, R.A. van den Heuvel, and A.A. van Gorkum, Appl. Phys. Lett. **57**, 2567 (1990).

[5] T.E. Whall, D.W. Smith, A.D. Plews, R.A. Kubiak, P.G. Phillips, and E.H.C. Parker, Semicond. Sci. Technol. **8**, 615 (1993).

[6] D.J. Paul, N. Griffin, D.D. Amone, M. Pepper, C.J. Emleus, P.G. Phillips, and T.E. Whall, Appl. Phys. Lett. **69**, 2704 (1996).

[7] E. Basaran, R.A. Kubiak, T.E. Whall, and E.H.C. Parker, Appl. Phys. Lett. **64**, 3470 (1994).

[8] T.E. Whall, J. Cryst. Growth **157**, 353 (1995).

[9] R.J.P. Lander, M.J. Kearney, A.I. Horrell, E.H.C. Parker, P.J. Phillips, and T.E. Whall, Semicond. Sci. Technol. **12**, 1604 (1997).

[10] C.J. Emeleus, T.E. Whall, D.W. Smith, R.A. Kubiak, E.H.C. Parker, and M.J. Kearney, J. Appl. Phys. **73**, 3852 (1993).

[11] D.R. Leadley, M.J. Kearney, A.I. Horrell, H. Fischer, L. Risch, E.C.H. Parker, and T.E. Whall, Semicond. Sci. Technol. **17**, 708 (2002).

[12] M.A. Sadeghzadeh, A.I. Horrell, O.A. Mironov, E.H.C. Parker, T.E. Whall, and M.J. Kearney, Appl. Phys. Lett. **76**, 2568 (2000).

[13] M.J. Kearney and A.I. Horrell, Semicond. Sci. Technol. **13**, 174 (1998).

[14] A.D. Plews, N.L. Mattey, P.J. Phillips, E.H.C. Parker, and T.E. Whall, Semicond. Sci. Technol. **12**, 1231 (1997).

[15] D.J. Srolovitz, Acta Metall. **37**, 621 (1989).

[16] R.M. Feenstra and M.A. Lutz, J. Appl. Phys. **78**, 6091 (1995).

[17] D.N. Quang, V.N. Tuoc, N.H. Tung, and T.D. Huan, Phys. Rev. Lett. **89**, 077601 (2002).

[18] D.N. Quang, V.N. Tuoc, and T.D. Huan, Phys. Rev. B **68**, 195316

(2003). There, the ordering of the powers from bottom to top along the ordinate axis of Fig. 1 was incorrectly printed and should be 10^0, 10^1, 10^2.
[19] D.N. Quang, V.N. Tuoc, N.H. Tung, and T.D. Huan, Phys. Rev. B **68**, 153306 (2003).
[20] R.M. Feenstra, M.A. Lutz, F. Stern, K. Ismail, P.M. Mooney, F.K. LeGoues, C. Stanis, J.O. Chu, and B.S. Meyerson, J. Vac. Sci. Technol. B **13**, 1608 (1995).
[21] Y.H. Xie, R. People, J.C. Bean, and K.W. Wecht, Appl. Phys. Lett. **49**, 283 (1986).
[22] Y.H. Xie, R. People, J.C. Bean, and K.W. Wecht, J. Vac. Sci. Technol. B **5**, 744 (1987).
[23] O.A. Mironov, V.I. Khizny, G. Braithwaite, E.H.C. Parker, P.J. Phillips, T.E. Whall, and V.P. Gnezdilov, J. Cryst. Growth **157**, 382 (1995).
[24] V.I. Khizhny, O.A. Mironov, E.H.C. Parker, P.J. Phillips, T.E. Whall, and M.J. Kearney, Appl. Phys. Lett. **69**, 960 (1996).
[25] T. Ando, A.B. Fowler, and F. Stern, Rev. Mod. Phys. **54**, 437 (1982).
[26] U. Ekenberg, W. Batty, and E.P. O'Reilly, J. Phys. Colloq. **48**, C5 (1987).
[27] J.M. Hinckley and J. Singh, Phys. Rev. B **41**, 2912 (1990).
[28] B. Laikhtman and R.A. Kiehl, Phys. Rev. B **47**, 10 515 (1993).
[29] T. Ando, J. Phys. Soc. Jpn. **51**, 3893 (1982); **51**, 3900 (1982).
[30] G. Bastard, *Wave Mechanics Applied to Semiconductor Heterostructures* (Les Editions de Physique, Paris, 1988).
[31] Y. Okuyama and N. Tokuda, Phys. Rev. B **40**, 9744 (1989).
[32] S.J. Manion, M. Artaki, M.A. Emanuel, J.J. Coleman, and K. Hess, Phys. Rev. B **35**, 9203 (1987).
[33] K. Schmalz, I.N. Yassievich, E.J. Collart, and D.J. Gravesteijn, Phys. Rev. B **54**, 16 799 (1996).
[34] U. Penner, H. Rücker, and I.N. Yassievich, Semicond. Sci. Technol. **13**, 709 (1998).
[35] M.J. Kearney and A.I. Horrell, Semicond. Sci. Technol. **14**, 211 (1999).
[36] A. Gold and W. Götze, J. Phys. C **14**, 4049 (1981); Phys. Rev. B **33**, 2495 (1986).
[37] F. Stern and W.E. Howard, Phys. Rev. **163**, 816 (1967).
[38] A. Gold, Phys. Rev. B **35**, 723 (1987).
[39] M. Jonson, J. Phys. C **9**, 3055 (1976).
[40] D.L. Smith and C. Mailhiot, Rev. Mod. Phys. **62**, 173 (1990).
[41] E. Anastassakis, Solid State Commun. **78**, 347 (1991).
[42] C. Herring and E. Vogt, Phys. Rev. **101**, 944 (1956).
[43] I. Balslev, Phys. Rev. **143**, 636 (1966).
[44] C.G. Van de Walle, Phys. Rev. B **39**, 1871 (1989).
[45] G.E. Pikus and G.L. Bir, Fiz. Tverd. Tela (Leningrad) **1**, 1642 (1959) [Sov. Phys. Solid State **1**, 1502 (1959)].
[46] G.L. Bir and G.E. Pikus, *Symmetry and Strain Induced Effects in Semiconductors* (Wiley, New York, 1974).
[47] J.P. Hirth and J. Lothe, *Theory of Dislocations* (Wiley, New York, 1982).
[48] C. Kittel, *Introduction to Solid State Physics*, 7th ed. (Wiley, New York, 1996).
[49] P. Harrison, *Quantum Wells, Wires, and Dots: Theoretical and Computational Physics* (Wiley, New York, 2000).
[50] R.A. Logan, J.M. Rowell, and F.A. Trumbore, Phys. Rev. **136**, A1751 (1964).
[51] M.V. Fischetti and S.E. Laux, J. Appl. Phys. **80**, 2234 (1996).
[52] V. Venkataraman, C.W. Liu, and J.C. Sturm, Appl. Phys. Lett. **63**, 2795 (1993).
[53] J.-P Cheng, V.P. Kesan, D.A. Grutzmacher, T.O. Sedgwick, and J.A. Ott, Appl. Phys. Lett. **62**, 1522 (1993).
[54] Y. Zhang and J. Singh, J. Appl. Phys. **83**, 4264 (1998).
[55] Y.H. Xie, G.H. Gilmer, C. Roland, P.J. Silverman, S.K. Buratto, J.Y. Cheng, E.A. Fitzgerald, A.R. Kortan, S. Schuppler, M.A. Marcus, and P.H. Citrin, Phys. Rev. Lett. **73**, 3006 (1994).
[56] J.F. Zheng, J.D. Walker, M.B. Salmeron, and E.R. Weber, Phys. Rev. Lett. **72**, 2414 (1994).
[57] T. Manku and A. Nathan, J. Appl. Phys. **69**, 8414 (1991).
[58] R. Oberhuber, G. Zandler, and P. Vogl, Phys. Rev. B **58**, 9941 (1998).
[59] H. Nakatsuji, Y. Kamakura, and K. Taniguchi, Tech. Dig. - Int. Electron Devices Meet. **2002**, 727.
[60] M.V. Fischetti, Z. Ren, P.M. Solomon, M. Yang, and K. Rim, J. Appl. Phys. **94**, 1079 (2003).